Title	FMO3-LCMO study of electron transfer coupling matrix element and pathway: Application to hole transfer between two tryptophans through cis- and trans-polyproline-linker systems
Author(s)	Kitoh-Nishioka, Hirotaka; Ando, Koji
Citation	The Journal of Chemical Physics (2016), 145(11)
Issue Date	2016-09-16
URL	http://hdl.handle.net/2433/216653
Right	Copyright 2016 AIP Publishing. This article may be downloaded for personal use only. Any other use requires prior permission of the author and AIP Publishing. The following article appeared in 'The Journal of Chemical Physics 145, 114103 (2016); doi: 10.1063/1.4962626' and may be found at http://scitation.aip.org/content/aip/journal/jcp/145/11/10.1063/1.4962626; The full-text file will be made open to the public on 16 September 2017 in accordance with publisher's 'Terms and Conditions for Self-Archiving'.
Type	Journal Article
Textversion	publisher

AIP | The Journal of Chemical Physics

FMO3-LCMO study of electron transfer coupling matrix element and pathway: Application to hole transfer between two tryptophans through cis- and trans-polyproline-linker systems

Hirotaka Kitoh-Nishioka and Koji Ando

Citation: The Journal of Chemical Physics **145**, 114103 (2016); doi: 10.1063/1.4962626
View online: http://dx.doi.org/10.1063/1.4962626
View Table of Contents: http://scitation.aip.org/content/aip/journal/jcp/145/11?ver=pdfcov
Published by the AIP Publishing

FMO3-LCMO study of electron transfer coupling matrix element and pathway: Application to hole transfer between two tryptophans through *cis*- and *trans*-polyproline-linker systems

Hirotaka Kitoh-Nishioka[a] and Koji Ando[b]
Department of Chemistry, Graduate School of Science, Kyoto University, Sakyo-ku, Kyoto 606-8502, Japan

(Received 18 June 2016; accepted 22 August 2016; published online 16 September 2016)

The linear-combination of fragment molecular orbitals with three-body correction (FMO3-LCMO) is examined for electron transfer (ET) coupling matrix elements and ET pathway analysis, with application to hole transfer between two tryptophans bridged by *cis*- and *trans*-polyproline linker conformations. A projection to the minimal-valence-plus-core FMO space was found to give sufficient accuracy with significant reduction of computational cost while avoiding the problem of linear dependence of FMOs stemming from involvement of bond detached atoms. *Published by AIP Publishing.* [http://dx.doi.org/10.1063/1.4962626]

I. INTRODUCTION

Long-distance electron transfer (ET) plays an essential role in biological energy conversion.[1–5] Representative is those in photosynthetic reaction centers in which photon energy is converted to electrochemical energy via series of ETs through redox centers embedded in transmembrane protein. A simple but fundamental question open to microscopic investigation is how the protein environment is involved in the ET; the protein structure could be involved passively by simply holding the redox centers at appropriate spatial configuration or actively by providing intermediate virtual states for superexchange ET mechanism.[6]

To address this and related questions, quantum mechanical investigation based on realistic molecular structure is essential. However, first-principles treatment of electrons in large biomolecular systems is still a formidable task. In this regard, fragment-based approaches, such as the fragment molecular orbital (FMO),[7–9] divide-and-conquer,[10,11] and many others[12–15] appear promising.

In a series of papers, we have reported calculations of ET coupling matrix element and ET pathways[16–18] from the linear-combination of FMOs (FMO-LCMO)[19] with the two-body correction (FMO2). The method was found to give accurate ET couplings over four orders of magnitude along the ET distance when the bond detached atoms (BDAs) were not involved or when the minimal atomic basis set was used.[16] Nevertheless, the problem of degraded MO energies caused by BDAs with atomic basis sets larger than minimal set, that had been already pointed out in Ref. 19, carried over to the ET analysis. Recently, however, Kobori *et al.* have found notable remedy of MO energies with the three-body correction (FMO3).[20] Following this, we study in this work how the FMO3 correction affects the ET coupling energy and ET pathway analysis.

We also examine selection of the FMO space. In Ref. 20, in order to remove linear dependence of basis functions associated with BDAs, a canonical transformation of Hamiltonian matrix,

$$\tilde{H} = U^{\dagger} H U, \tag{1}$$

where the matrix U diagonalizes overlap matrix, was employed. However, this transformation often mixes the FMOs in unwanted ways for the ET pathway analysis, particularly for studying inter-fragment tunneling current. We found that the problem can be evaded by a projection to restricted FMO (rFMO) space instead of the canonical transformation of Eq. (1). For instance, with FMO-LC(VC)MO scheme, which restricts to the minimal-valence (V) plus core (C) MO space, the smallest eigenvalue of overlap matrix for systems studied in this work was 0.225, which is large enough to regard the FMO space linearly independent.[21]

For numerical demonstration, we examine hole transfer between two tryptophan (Trp) residues bridged by helical polyproline (PP) oligopeptide, which serves as a good model of long-distance ETs observed in metal-derivatized oligoprolines.[22–24] Previous theoretical works[25,26] have employed the same model systems to study the effects of solvent and bridge-conformation dynamics on the electronic coupling.

Section II outlines the theoretical framework. Section III describes the computational details. Applications to hole transfer between two Trp molecules bridged by polyproline linker systems are discussed in Sec. IV. Section V concludes.

II. THEORY

A. FMO-LCMO and projection to restricted FMO space

Here we outline the FMO-LCMO method[19,20] to explain the present projection scheme to the restricted FMO space.

The FMO-LCMO Hamiltonian up to the three-body FMO3 correction is described as

$$H_{\text{total}}^{\text{FMO3}} = H_{\text{total}}^{\text{FMO1}} + \Delta H_{\text{total}}^{\text{FMO2}} + \Delta H_{\text{total}}^{\text{FMO3}}, \tag{2}$$

[a]Present address: Center for Computational Sciences, University of Tsukuba. Electronic mail: hkito@ccs.tsukuba.ac.jp
[b]E-mail: ando@kuchem.kyoto-u.ac.jp

in which $H^{\mathrm{FMO1}}_{\mathrm{total}}$ consists of monomer Fock matrices, and $\Delta H^{\mathrm{FMO2}}_{\mathrm{total}}$ and $\Delta H^{\mathrm{FMO3}}_{\mathrm{total}}$ are the two- and three-body corrections. The intra-fragment block of $\Delta H^{\mathrm{FMO2}}_{\mathrm{total}}$, between FMOs ϕ^I_p and ϕ^I_q in the same fragment I, is given by

$$(\Delta H^{\mathrm{FMO2}}_{\mathrm{total}})_{I_p,I_q} = \sum_{J\neq I}\{(H_{I\leftarrow IJ})_{I_p,I_q} - (H_{I\leftarrow I})_{I_p,I_q}\}, \quad (3)$$

whereas the inter-fragment block is

$$(\Delta H^{\mathrm{FMO2}}_{\mathrm{total}})_{I_p,J_q} = (H_{IJ\leftarrow IJ})_{I_p,J_q}. \quad (4)$$

The terms in the right-hand-side of Eqs. (3) and (4) will be defined in Eqs. (7)–(9).

The FMO3 correction to the intra- and inter-fragment blocks is

$$(\Delta H^{\mathrm{FMO3}}_{\mathrm{total}})_{I_p,I_q} = \sum_{J<K}\sum_{J,K\neq I}\{(H_{I\leftarrow IJK})_{I_p,I_q} - (H_{I\leftarrow IJ})_{I_p,I_q} - (H_{I\leftarrow IK})_{I_p,I_q} + (H_{I\leftarrow I})_{I_p,I_q}\} \quad (5)$$

and

$$(\Delta H^{\mathrm{FMO3}}_{\mathrm{total}})_{I_p,J_q} = \sum_{K\neq I,J}\{(H_{IJ\leftarrow IJK})_{I_p,J_q} - (H_{IJ\leftarrow IJ})_{I_p,J_q}\}. \quad (6)$$

As noted in Introduction, the canonical transformation of Eq. (1) is not desired for the ET pathway analysis. We thus simply limit the number of FMOs and project the Hamiltonian matrix to this set. We denote this as "restricted FMO (rFMO)" space. Therefore, the terms in the right-hand-side of Eqs. (3)–(6) in the selected rFMO space $\{\phi^I_p\}$ are defined as follows. With the fragment monomer, dimer (DIM), and trimer represented by $X = I, IJ$, and IJK, the intra-fragment blocks are defined by

$$(H_{I\leftarrow I})_{I_p,I_q} = \varepsilon_{I_p}\delta_{I_p,I_q} \quad (7)$$

and

$$(H_{I\leftarrow X})_{I_p,I_q} = \sum_{X_r}\langle\phi^I_p|\phi^X_r\rangle\varepsilon^X_r\langle\phi^X_r|\phi^I_q\rangle, \quad (8)$$

whereas the inter-fragment blocks are

$$(H_{IJ\leftarrow X})_{I_p,J_q} = \sum_{X_r}\langle\phi^I_p|\phi^X_r\rangle\varepsilon^X_r\langle\phi^X_r|\phi^J_q\rangle. \quad (9)$$

In the summation over X_r in the right-hand-side, all the dimer and trimer FMOs are taken, except the spurious ones stemming from the BDAs.

B. ET coupling and pathway analysis

To calculate the ET coupling matrix element T_{DA}, we employ two methods: generalized Mulliken-Hush (GMH)[27] and bridge Green function (BGF).[28–30]

The GMH method scales the donor-acceptor MO energy splitting $\Delta\varepsilon_{\mathrm{DA}}$ by a formula

$$T_{\mathrm{DA}} = \frac{|\mu_{\mathrm{DA}}|\,\Delta\varepsilon_{\mathrm{DA}}}{\sqrt{(\mu_{\mathrm{D}}-\mu_{\mathrm{A}})^2 + 4|\mu_{\mathrm{DA}}|^2}}, \quad (10)$$

in which μ_{D}, μ_{A}, and μ_{DA} are the diagonal and off-diagonal dipole matrix elements. It assumes that the Hamiltonian and dipole matrix elements scale similarly for states involved in ETs. Despite its simplicity, the GMH formula (10) has been successfully applied to a number of ET reactions.

The BGF method has been also demonstrated to give accurate and robust results with

$$T_{\mathrm{DA}} = H^{\mathrm{direct}}_{\phi_{\mathrm{D}},\phi_{\mathrm{A}}} + \sum_{I,J}{\sum_{I_p,J_q}}'(E_{\mathrm{tun}}S_{\phi_{\mathrm{D}},I_p} - H_{\phi_{\mathrm{D}},I_p}) \times G^{\mathrm{B}}(E_{\mathrm{tun}})_{I_p,J_q}(E_{\mathrm{tun}}S_{J_q,\phi_{\mathrm{A}}} - H_{J_q,\phi_{\mathrm{A}}}), \quad (11)$$

in which the sums over I_p and J_q exclude donor and acceptor MOs, ϕ_{D} and ϕ_{A}. The first term in the right-hand-side is the direct coupling between ϕ_{D} and ϕ_{A}. S is the overlap matrix. $G^{\mathrm{B}}(E)$ is the bridge Green function defined as

$$G^{\mathrm{B}}(E) = (ES_{QQ} - H_{QQ})^{-1}, \quad (12)$$

in which Q is the projection operator to the MO space external to the donor-acceptor MOs. The electron tunneling energy E_{tun} is naturally defined as the average of donor-acceptor orbital energies, $E_{\mathrm{tun}} = (\varepsilon_{\mathrm{D}} + \varepsilon_{\mathrm{A}})/2$.

In the tunneling current analysis,[30,31] the ET coupling T_{DA} is expressed as a sum of tunneling current $\mathcal{J}_{I_p,J_q}$ between basis FMOs $\{\phi^I_p\}$,[16,17]

$$T_{\mathrm{DA}} = \hbar\sum_{I\in\Omega_{\mathrm{D}}}\sum_{J\notin\Omega_{\mathrm{D}}}\mathcal{J}_{I,J}, \quad (13)$$

$$\mathcal{J}_{I,J} = \sum_{I_p}\sum_{J_q}\mathcal{J}_{I_p,J_q}, \quad (14)$$

in which the summation over I_p and J_q is over the FMOs within fragments I and J, and Ω_{D} denotes the spatial region assigned to the donor molecule. The inter-orbital current $\mathcal{J}_{I_p,J_q}$ is computed from the electronic Hamiltonian and overlap matrices and the coefficients of FMO-LCMO, $\{C^{\mathrm{i}}_{I_p}\}$ and $\{C^{\mathrm{f}}_{I_p}\}$, that represent the mixing of bridge FMOs to the donor and acceptor FMOs, ϕ_{D} and ϕ_{A}, in the initial (i) and final (f) states, ψ^{i} and ψ^{f},

$$|\psi^{\mathrm{i}}\rangle = C^{\mathrm{i}}_{\mathrm{D}}|\phi_{\mathrm{D}}\rangle + \sum_{I}^{N}\sum_{I_p}C^{\mathrm{i}}_{I_p}|\phi^I_p\rangle, \quad (15)$$

$$|\psi^{\mathrm{f}}\rangle = C^{\mathrm{f}}_{\mathrm{A}}|\phi_{\mathrm{A}}\rangle + \sum_{I}^{N}\sum_{I_p}C^{\mathrm{f}}_{I_p}|\phi^I_p\rangle, \quad (16)$$

$$\mathcal{J}_{I_p,J_q} = \frac{1}{\hbar}\left(H_{I_p,J_q} - E_{\mathrm{tun}}S_{I_p,J_q}\right)\left(C^{\mathrm{i}}_{I_p}C^{\mathrm{f}}_{J_q} - C^{\mathrm{f}}_{I_p}C^{\mathrm{i}}_{J_q}\right). \quad (17)$$

These are thus computed straightforwardly from the FMO-LCMO method. The normalized inter-fragment tunneling current is defined by

$$\mathcal{K}_{I,J} = \hbar\mathcal{J}_{I,J}/T_{\mathrm{DA}}, \quad (18)$$

which satisfies

$$\sum_{I\in\Omega_{\mathrm{D}},J\notin\Omega_{\mathrm{D}}}\mathcal{K}_{I,J} = 1. \quad (19)$$

III. COMPUTATION

A. Polyproline linker conformation

For the purpose of benchmarking the FMO3-LCMO calculations, we consider proline-trimer bridged systems, Trp-$(Pro)_3$-Trp, with two types of helix structure of polyproline (PP) linker, one with *cis*-configurations (*cis*PP) and the other with *trans*-configurations (*trans*PP) of peptide bonds. The former and latter proline trimers have the backbone dihedral angles (φ,ψ) of approximately $(-75°, 150°)$ and $(-75°, 160°)$, respectively. The *cis*PP and *trans*PP structures are schematically drawn in Fig. 1. Apparently the *trans*PP is more stretched.

Starting from typical conformations of *cis*PP and *trans*PP, local strains were removed by geometry optimization at the B3LYP/6-31G(d)-D3 level, with the D3 version of Grimme's dispersion correction with the original D3 damping function.[32] We used Gaussian09 program[33] for the geometry optimization. The resultant molecular structures are displayed in Fig. S1 and Table S1 of the supplementary material.

B. FMO calculation

In the FMO calculation, the Trp-$(Pro)_3$-Trp chain was divided into six fragments as designated in Fig. 2, in which P1-P3 are the three prolines and MW denotes the main-chain of Trp (W). The α-carbon atoms were treated as BDAs. The HOMOs of Trp fragments were taken as the donor and acceptor MOs of hole transfer. The electronic coupling and tunneling current from the FMO2-LCMO and FMO3-LCMO methods were compared to a reference calculation with the restricted Hartree-Fock (RHF) Hamiltonian of the entire system of six fragments projected to the FMO space. We denote this last scheme FMO6-LCMO with the Hamiltonian matrix

$$(H^{\mathrm{FMO6}}_{\mathrm{total}})_{I_p,J_q} = \sum_a \langle \phi^I_p|\psi_a\rangle \varepsilon_a \langle \psi_a|\phi^J_q\rangle, \tag{20}$$

where ϕ^I_p and ϕ^I_q are MOs in the rFMO space and ψ_a and ε_a are the MOs and MO energies of the entire system.

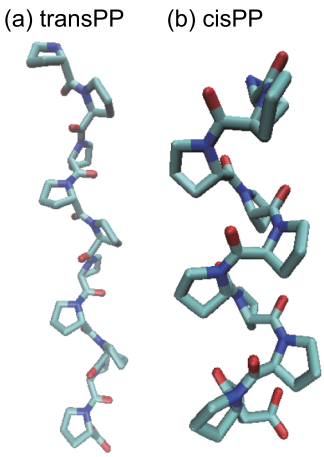

FIG. 1. Schematic drawings of the helix structures of polyproline linker with (a) *trans*- and (b) *cis*-configurations.

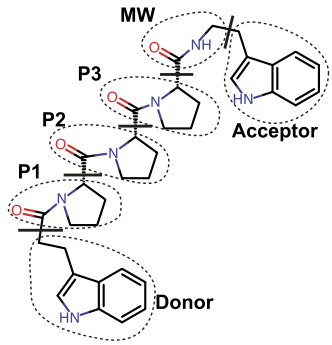

FIG. 2. Fragments in polyproline linker. P1-3 are three proline residues and MW denotes the main chain of Trp (W).

We consider a "minimal-valence plus core" rFMO space that includes the same number of MOs as the minimal basis set such as STO-3G. We denote this as LC(VC)MO space. Other choices of rFMO space, LUMO, LUMO+2, LUMO+6, LUMO+10, to check the dependence on the size of rFMO space, are obtained by augmenting the lower unoccupied MOs of each fragment to the occupied space.

The 6-31G(d) basis set was used. The total number of basis AOs for the entire system is 774. The FMO2 and FMO3 calculations include additional 50 AOs from the BDAs. The number of FMOs in the occupied, LC(VC)MO, and full spaces for each fragment is summarized in Table I. For basis sets larger than the double-zeta basis, the LC(VC)MO scheme gives significant reduction. Moreover, it removed the problem of linear-dependence observed previously,[20] as the smallest eigenvalue of the overlap matrix in the LC(VC)MO space was 0.225.

We used the program GAMESS[34] for the conventional FMO calculation.[35] To estimate all inter-fragment tunneling currents including the long-distance ones, we did not employ the electrostatic dimer (ES-DIM) approximation[36] that avoids self-consistent field calculations of the far separated dimers in FMO calculations.

TABLE I. Number of MOs in the rFMO spaces.

	D	P1	P2	P3	MW	A	Total
Occupied	38	26	26	26	15	35	166
LC(VC)MO	64	42	42	42	23	59	272[a]
Full	184	129	129	129	76	177	824 (774[b])

[a]Corresponds to the minimal set.
[b]Without BDAs.

TABLE II. MO energy gap and errors (in eV) of *trans*PP helix from FMO-LC(VC)MO calculations.

		MAE[b]		RMS[c]	
	Gap[a]	Occ	Uoc	Occ	Uoc
FMO2	10.66	0.107 (#15)	22.4 (#272)	0.0345	3.92
FMO3	10.67	0.102 (#27)	14.6 (#272)	0.0266	3.13
FMO6	10.63	0.0934 (#65)	14.6 (#272)	0.0223	3.13

[a]HOMO-LUMO gap. The reference RHF value is 10.63 eV.
[b]Maximum absolute error of MO energies. Occ / Uoc denote occupied / unoccupied MOs. In parentheses are the MO numbers that exhibit the MAE.
[c]Root-mean-square error of MO energies.

TABLE III. Same as Table II but for *cis*PP helix.

		MAE		RMS	
	Gap[a]	Occ	Uoc	Occ	Uoc
FMO2	9.885	0.271 (#19)	22.18 (#272)	0.0504	3.74
FMO3	9.890	0.0988 (#40)	14.89 (#272)	0.0227	3.12
FMO6	9.909	0.0863 (#65)	14.95 (#272)	0.0213	3.14

[a]The reference RHF value is 9.904 eV.

IV. RESULTS

A. Errors in MO energy

The diagonalization of the FMO-LCMO Hamiltonian matrix can provide approximate canonical MOs and corresponding energies for the entire system.[19,20] First we assess accuracy of the FMO-LC(VC)MO method with regard to the MO energies. The computed errors from the RHF calculation of the entire system are summarized in Tables II and III for *trans*PP and *cis*PP, respectively. For the occupied MOs, the maximum absolute error (MAE) was observed at different MO numbers for FMO2, FMO3, and FMO6 calculations (for instance, Nos. 15, 27, and 65 for *trans*PP) but these commonly involve the BDA. The MAE of unoccupied MOs was always observed at the highest MO (No. 272). The root-mean-square error is notably reduced from FMO2 to FMO3 but not so much from FMO3 to FMO6, indicating nearly converged accuracy at the FMO3 level.

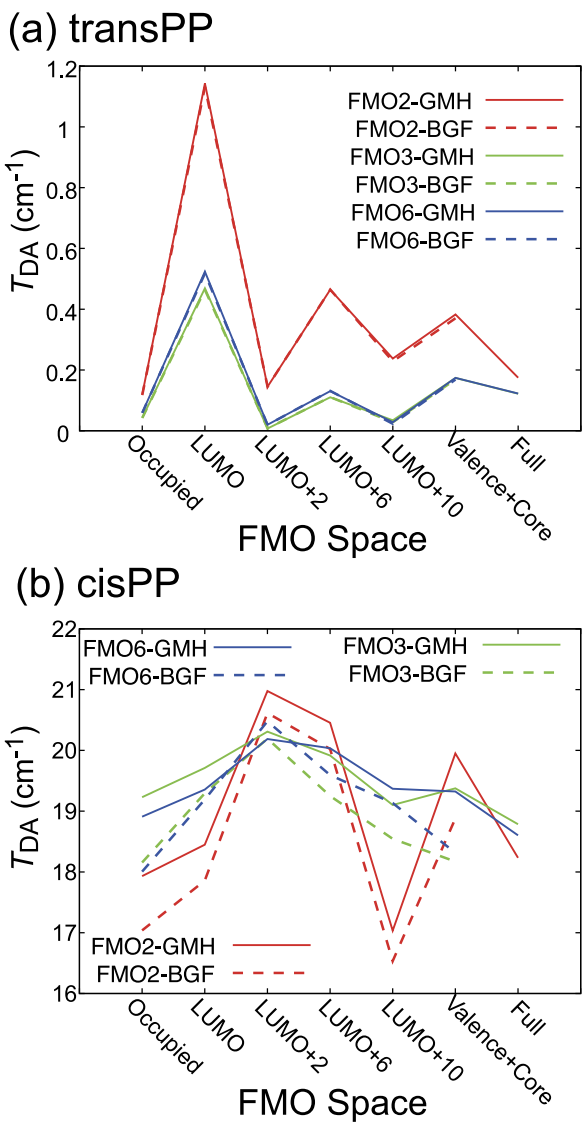

FIG. 3. Transfer matrix element T_{DA} with various rFMO spaces for (a) *trans*PP and (b) *cis*PP.

TABLE IV. Transfer matrix element T_{DA} (in cm^{-1}) with various rFMO spaces for *trans*PP complex.

	FMO2		FMO3		FMO6	
FMO space	GMH	BGF	GMH	BGF	GMH	BGF
Full	0.1745	...	0.121 9	...	0.122 4	...
LC(VC)MO	0.3826	0.3702	0.173 8	0.168 8	0.174 0	0.168 7
LUMO+10	0.2375	0.2286	0.034 38	0.028 50	0.028 06	0.023 01
LUMO+6	0.4642	0.4646	0.110 1	0.110 8	0.130 3	0.131 2
LUMO+2	0.1451	0.1448	0.073 64	0.079 56	0.020 0	0.019 5
LUMO	1.143	1.132	0.464 1	0.463 8	0.523 8	0.517 6
Occupied	0.1198	0.1173	0.042 52	0.041 99	0.059 32	0.058 58

B. ET coupling energy

Next we examine the ET coupling matrix element T_{DA}. Figure 3 displays the computed T_{DA} with varying rFMO spaces, from the "occupied-only" to the minimal-valence plus core (VC). The numerical values are listed in Tables IV and V. The absolute value of T_{DA} is about 20 times larger for *cis*PP than *trans*PP because of the shorter donor-acceptor distance in the former. As seen in Fig. 3(a), the T_{DA} in *trans*PP converge to the value of full space with an oscillation. The behavior for *cis*PP in Fig. 3(b) is less simple; the results of FMO2 exhibit notable oscillation which is less prominent in FMO3 and FMO6. For both *cis*PP and *trans*PP, FMO3 notably improves the T_{DA} value over FMO2 and has been almost converged to FMO6.

Interestingly, the results with the occupied space appear closest to those with the full FMO space. We consider this as the hole transfer is the principal mechanism for the present system. Thus, the addition of small number of LUMOs could have caused imbalance of description. However, generality of this view should be examined with more cases.

TABLE V. Same as Table IV but for *cis*PP complex.

	FMO2		FMO3		FMO6	
	GMH	BGF	GMH	BGF	GMH	BGF
Full	18.23	...	18.79	...	18.60	...
LC(VC)MO	19.95	18.88	19.38	18.17	19.32	18.31
LUMO+10	17.03	16.53	19.10	18.54	19.37	19.13
LUMO+6	22.45	20.02	19.92	19.25	20.04	19.59
LUMO+2	29.98	20.61	20.31	20.19	20.19	20.48
LUMO	18.45	17.86	19.71	19.29	19.36	19.19
Occupied	17.93	17.04	19.23	18.16	18.91	18.01

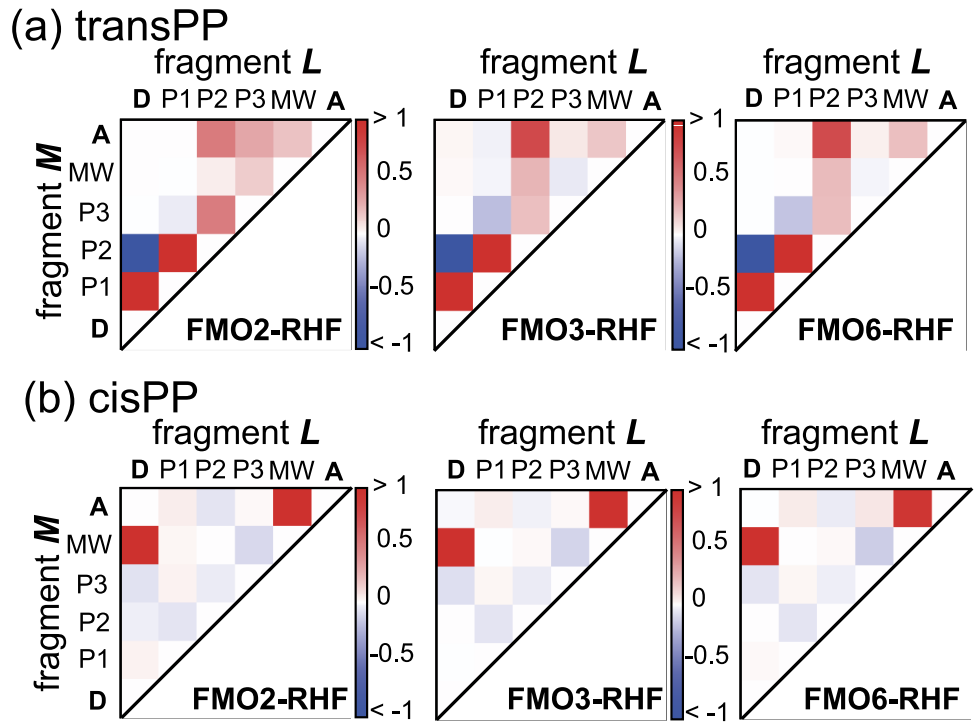

FIG. 4. Normalized inter-fragment tunneling current $\mathcal{K}_{L,M}$ from fragment L to M with FMO2-, FMO3-, and FMO6-LC(VC)MO methods for (a) *trans*PP and (b) *cis*PP.

C. ET pathway analysis

Now we examine the ET pathway. Figure 4(a) displays the normalized inter-fragment tunneling currents in *trans*PP, comparing FMO2 and FMO3 with the reference FMO6. In this figure, the LC(VC)MO space was employed. The numerical values are listed in Tables S8-S10 of the supplementary material. The figure clearly indicates improvement of accuracy with FMO3 over FMO2. The main pathway is the forward ET of D→P1→P2→A, with a bifurcate back-flow of P2→D. The back-flow is due to destructive interference. (See Eq. (13).) The figure indicates that FMO3 and FMO6 exhibit larger back-flow than FMO2, which explains the overestimate of T_{DA} by FMO2 seen in Fig. 3(a).

The corresponding results for *cis*PP are displayed in Fig. 4(b). The numerical values are listed in Tables S11-S13 of the supplementary material. The major pathway is the forward flow of D→MW→A. In contrast with *trans*PP, both FMO2 and FMO3 qualitatively reproduce the pathway of reference FMO6 calculation. This implies that as noted in Sec. IV B, the shorter donor-acceptor distance in *cis*PP makes the direct pathway dominant, which could have masked the error stemming from the BDAs.

V. CONCLUDING REMARKS

Comparison between *cis*PP and *trans*PP indicated that the value of T_{DA} is affected notably by the selection of rFMO space. Generally, the three-body correction of FMO3 markedly improved the T_{DA} value. The ET pathway analysis is also made robust by the FMO3 correction, especially when the BDAs are involved in the ET pathway.

We employed the restricted Hartree-Fock (RHF) wave function in this first report. To include electron correlation effects, an efficient way would be with the density functional theory. For instance, we have recently found that the Kohn-Sham orbitals from the long-range corrected functional give accurate electronic coupling energies with non-empirical tuning of the range-separation parameter.[18] The FMO3 correction will also make this scheme versatile. To the correlated wave functions such as the configuration interaction and coupled-cluster, extension of the FMO-LCMO scheme seems less straightforward but deserves further examination.

SUPPLEMENTARY MATERIAL

See the supplementary material for the optimized structures, MO energies and errors for various rFMO spaces, and the numerical values for Fig. 4.

ACKNOWLEDGMENTS

The authors acknowledge support from KAKENHI No. 20108017 ("π-space"). H.K.-N. also acknowledges support from Collaborative Research Program for Young Scientists of ACCMS and IIMC, Kyoto University.

[1]C. C. Moser, J. M. Keske, K. Warncke, R. S. Farid, and P. L. Dutton, Nature **355**, 796 (1992).
[2]P. L. Dutton and C. C. Mosser, Proc. Natl. Acad. Sci. U. S. A. **91**, 10247 (1994).
[3]J. R. Winkler, A. J. Di Bilio, N. A. Farrow, J. H. Richards, and H. B. Gray, Pure Appl. Chem. **71**, 1753 (1999).
[4]H. B. Gray and J. R. Winkler, Proc. Natl. Acad. Sci. U. S. A. **102**, 3534 (2005).
[5]O. Farver and I. Pecht, Coord. Chem. Rev. **255**, 757 (2011).

[6]H. M. McConnell, J. Chem. Phys. **35**, 508 (1961).
[7]K. Kitaura, E. Ikeo, T. Asada, T. Nakano, and M. Uebayasi, Chem. Phys. Lett. **313**, 701 (1999).
[8]D. G. Fedorov and K. Kitaura, J. Phys. Chem. A **111**, 6904 (2007).
[9]S. Tanaka, Y. Mochizuki, Y. Komeiji, Y. Okiyama, and K. Fukuzawa, Phys. Chem. Chem. Phys. **16**, 10310 (2014).
[10]W. Yang and T. S. Lee, J. Chem. Phys. **103**, 5674 (1995).
[11]T. Akama, M. Kobayashi, and H. Nakai, Int. J. Quantum Chem. **109**, 2706 (2009).
[12]W. Li and P. Piecuch, J. Phys. Chem. A **114**, 6721 (2010).
[13]Y. Aoki and F. L. Gu, Phys. Chem. Chem. Phys. **14**, 7640 (2012).
[14]M. S. Gordon, D. G. Fedorov, S. R. Pruitt, and L. V. Slipchenko, Chem. Rev. **112**, 632 (2012).
[15]K. Raghavachari and A. Saha, Chem. Rev. **115**, 5643 (2015).
[16]H. Nishioka and K. Ando, J. Chem. Phys. **134**, 204109 (2011).
[17]H. Kitoh-Nishioka and K. Ando, J. Phys. Chem. B **116**, 12933 (2012).
[18]H. Kitoh-Nishioka and K. Ando, Chem. Phys. Lett. **621**, 96 (2015).
[19]S. Tsuneyuki, T. Kobori, K. Akagi, K. Sodeyama, K. Terakura, and H. Fukuyama, Chem. Phys. Lett. **476**, 104 (2009).
[20]T. Kobori, K. Sodeyama, T. Otsuka, Y. Tateyama, and S. Tsuneyuki, J. Chem. Phys. **139**, 094113 (2013).
[21]A. Szabo and N. S. Ostlund, *Modern Quantum Chemistry* (Dover, New York, 1996).
[22]S. S. Isied, M. Y. Ogawa, and J. F. Wishart, Chem. Rev. **92**, 381 (1992).
[23]M. Y. Ogawa, J. F. Wishart, Z. Young, J. R. Miller, and S. S. Isied, J. Phys. Chem. **97**, 11456 (1993).
[24]M. Y. Ogawa, I. Moreira, J. F. Wishart, and S. S. Isied, Chem. Phys. **176**, 589 (1993).
[25]F. Wallrapp, A. A. Voityuk, and V. Guallar, J. Chem. Theory Comput. **5**, 3312 (2009).
[26]F. Wallrapp, A. A. Voityuk, and V. Guallar, J. Chem. Theory Comput. **6**, 3241 (2010).
[27]R. J. Cave and M. D. Newton, Chem. Phys. Lett. **249**, 15 (1996).
[28]S. S. Skourtis and D. N. Beratan, Adv. Chem. Phys. **106**, 377 (1999).
[29]J. J. Regan and J. N. Onuchic, Adv. Chem. Phys. **107**, 497 (1999).
[30]A. A. Stuchebrukhov, Theor. Chem. Acc. **110**, 291 (2003).
[31]A. A. Stuchebrukhov, J. Chem. Phys. **105**, 10819 (1996).
[32]S. Grimme, J. Antony, S. Ehrlich, and H. Krieg, J. Chem. Phys. **132**, 154104 (2010).
[33]M. J. Frisch, G. W. Trucks, H. B. Schlegel, G. E. Scuseria, M. A. Robb, J. R. Cheeseman, G. Scalmani, V. Barone, B. Mennucci, G. A. Petersson *et al.*, GAUSSIAN 09, Revision D.01, Gaussian, Inc., Wallingford, CT, 2013.
[34]M. W. Schmidt, K. K. Baldridge, J. A. Boatz, S. T. Elbert, M. S. Gordon, J. H. Jensen, S. Koseki, N. Matsunaga, K. A. Nguyen, S. Su *et al.*, J. Comput. Chem. **14**, 1347 (1993).
[35]D. G. Fedorov and K. Kitaura, J. Chem. Phys. **120**, 6832 (2004).
[36]T. Nakano, T. Kaminuma, T. Sato, K. Fukuzawa, Y. Akiyama, M. Uebayasi, and K. Kitaura, Chem. Phys. Lett. **351**, 475 (2002).